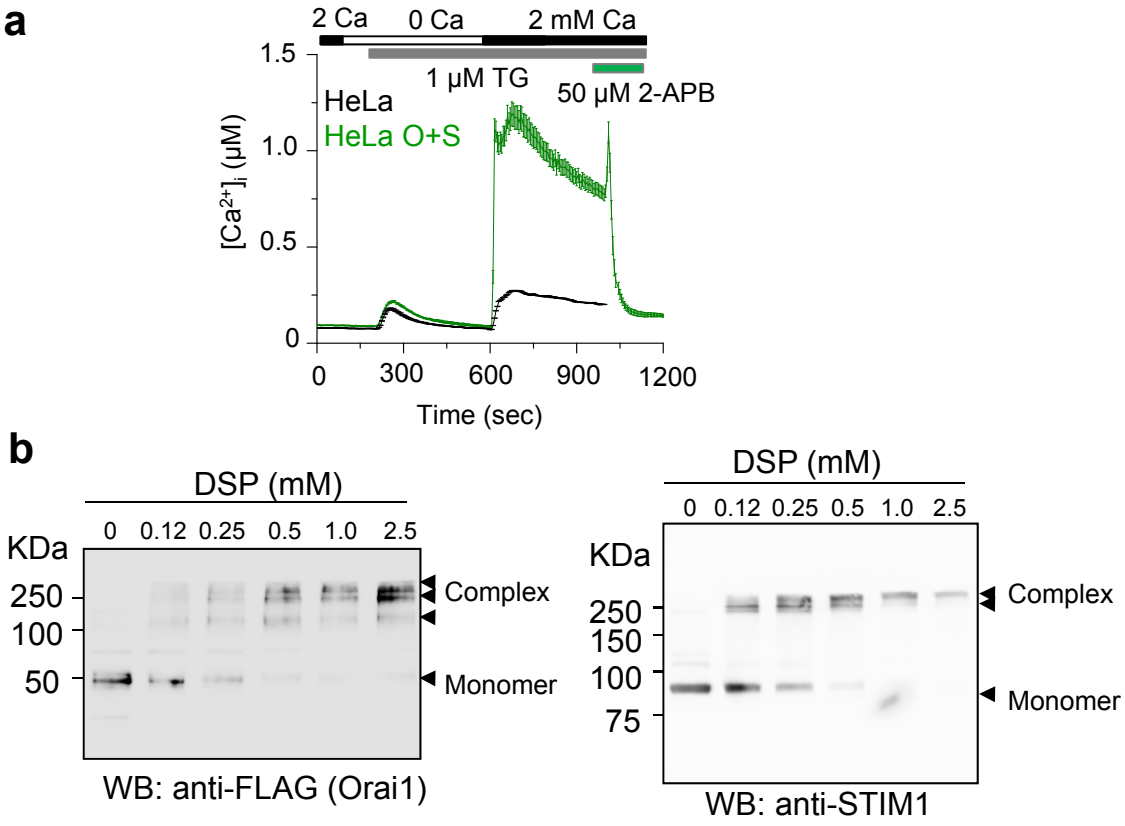

Figure S1 Measurement of store-operated Ca^{2+} entry (SOCE) in HeLa O+S cells and detection of high MW protein complexes containing Orai1 and STIM1 by DSP cross-linking. (**a**) Control HeLa cells or HeLa cells stably expressing Orai1 and STIM1 (HeLa O+S) were examined for SOCE. Inhibition of CRAC channel activity was monitored using 2-APB (50 μM). Each trace represents average ± s.e.m from 50-60 cells. (**b**) HeLa O+S cells were treated with different concentrations of DSP for one hour. Cell lysates were cleared by ultracentrifugation and analyzed by non-reducing SDS-PAGE and immunoblotted with anti-FLAG (Orai1, left) or anti-STIM1 (right) antibodies.

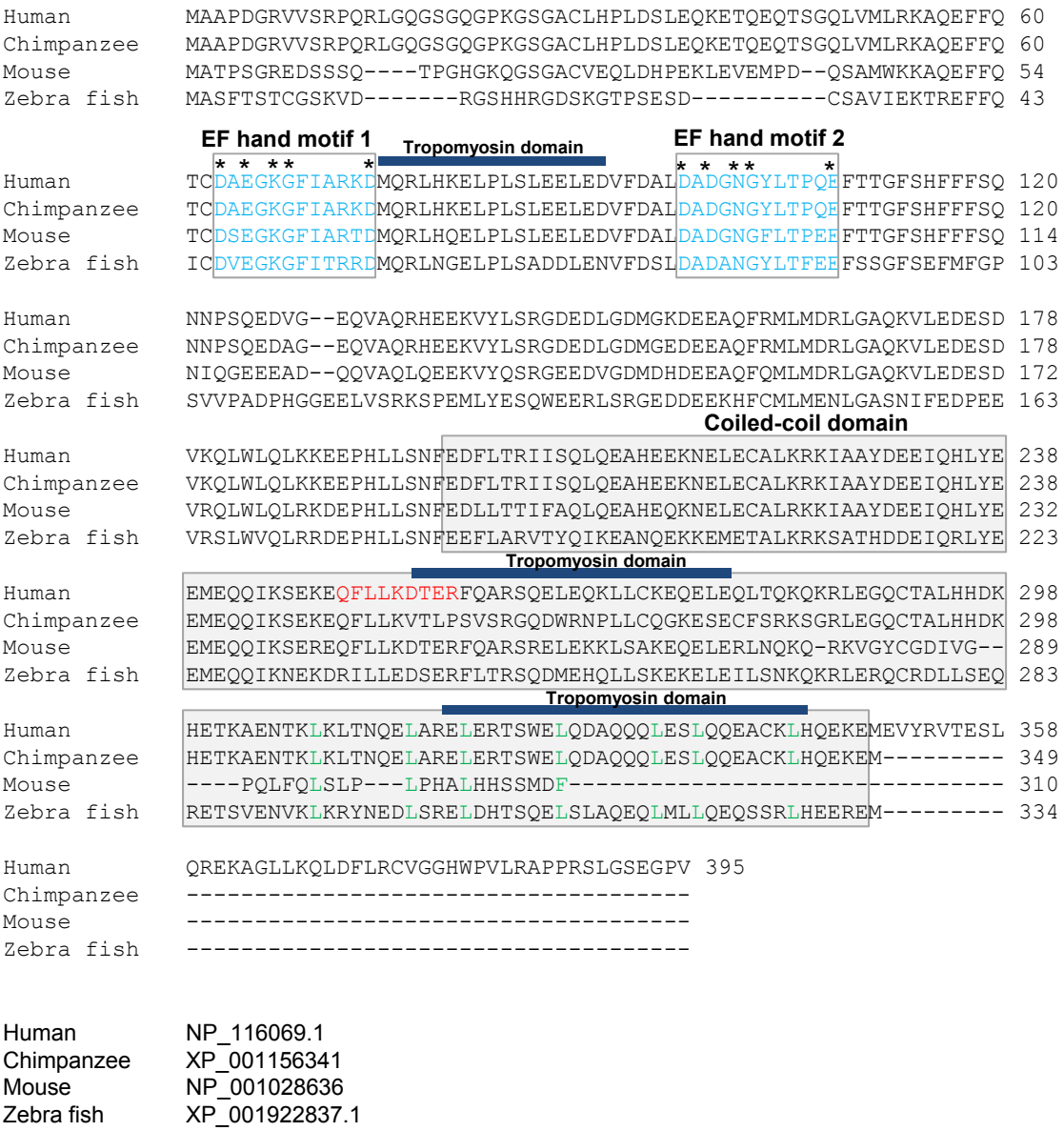

Figure S2 Amino acid sequence alignment of CRACR2A from various species. Amino acid sequences of human, chimpanzee, mouse and zebrafish CRACR2A proteins were aligned using ClustalW2 (default options). The predicated conserved EF-hands are colored in light blue (predicted using SMART). The predicted coiled-coil sequence (Human Protein Reference Database and COILS) in the C terminus is boxed in gray and tropomyosin domains predicted using PRINTS are highlighted in blue. The CRACR2A peptide detected from mass spectrometry is shown in red. This peptide was detected in a gel fragment corresponding to MW of ~45 kDa as described in Fig. 1. In humans, three alternative transcripts of CRACR2A (NM_001144958.1, NM_001144959.1 and NM_032680.3) were identified. Proteins derived from three isoforms are identical in their first 372 amino acids with differences in their C-terminal sequences. Amino acids sequences corresponding to isoform c of CRACR2A (predicted MW; 45.6 kDa, Compute pI/Mw tool) have been aligned here.

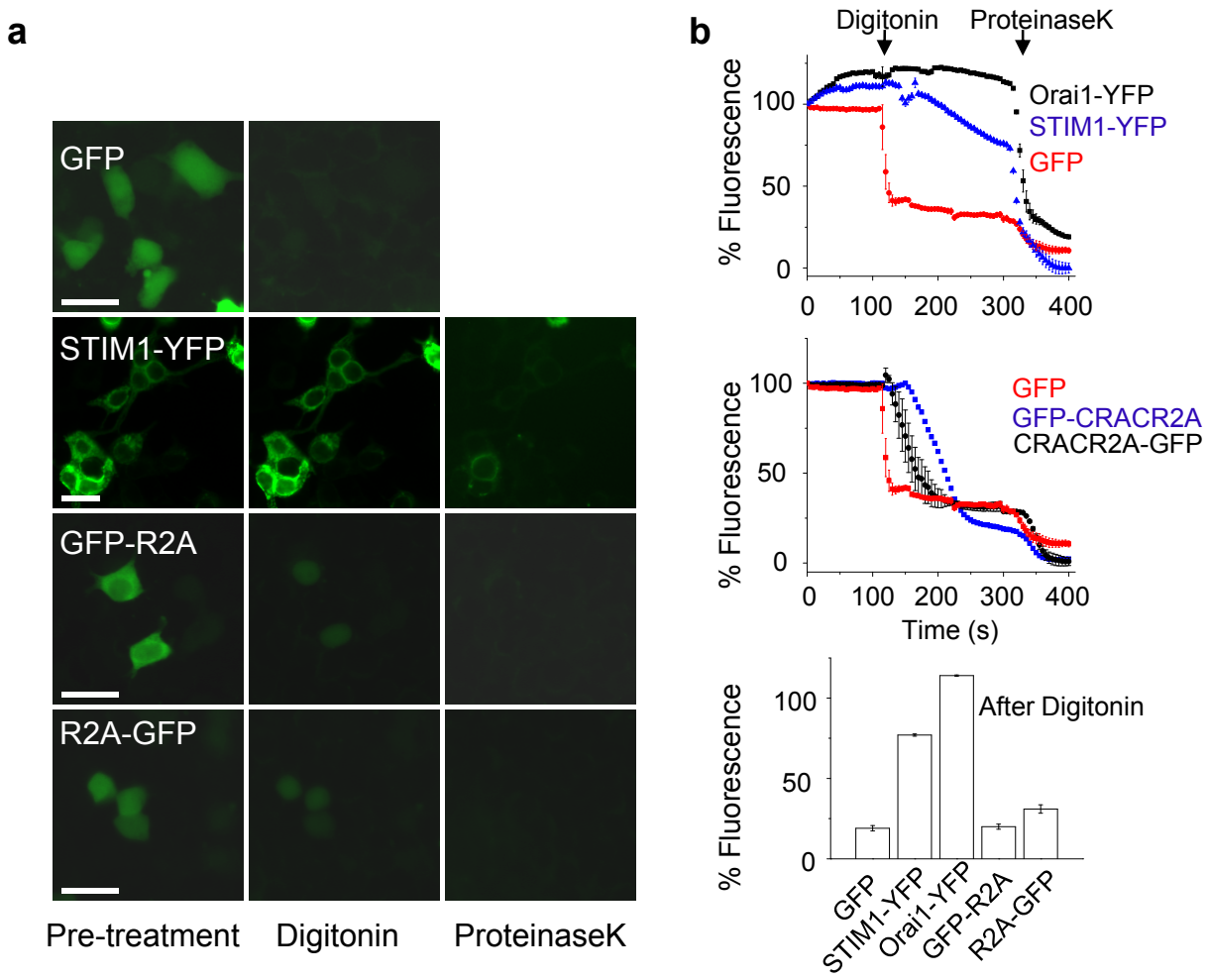

Figure S3 CRACR2A is a cytosolic protein as judged by fluorescence protease protection (FPP) assay. (**a**) HEK293 cells expressing either N- or C-terminally GFP-tagged CRACR2A proteins were treated with digitonin to permeabilize the cells and allow for diffusion of cytoplasmic proteins outside the cell. Subsequent treatment of cells with proteinase K leads to degradation of GFP tags exposed to the cytoplasm and thereby reduction in fluorescence. STIM1-YFP and Orai1-YFP used as controls for proteins integral to the ER and plasma membrane respectively, showed reduction in fluorescence upon proteinase K treatment (top graph) due to cytoplasmic localization of their YFP tags. Bar, 20 μm (**b**) Graphical representation of the images shown in panel a. The initial intensity of fluorescence was set to 100%. Each trace represents average ± s.e.m from 30-50 individual cells. The bar graph shows average ± s.e.m from three different experiments.

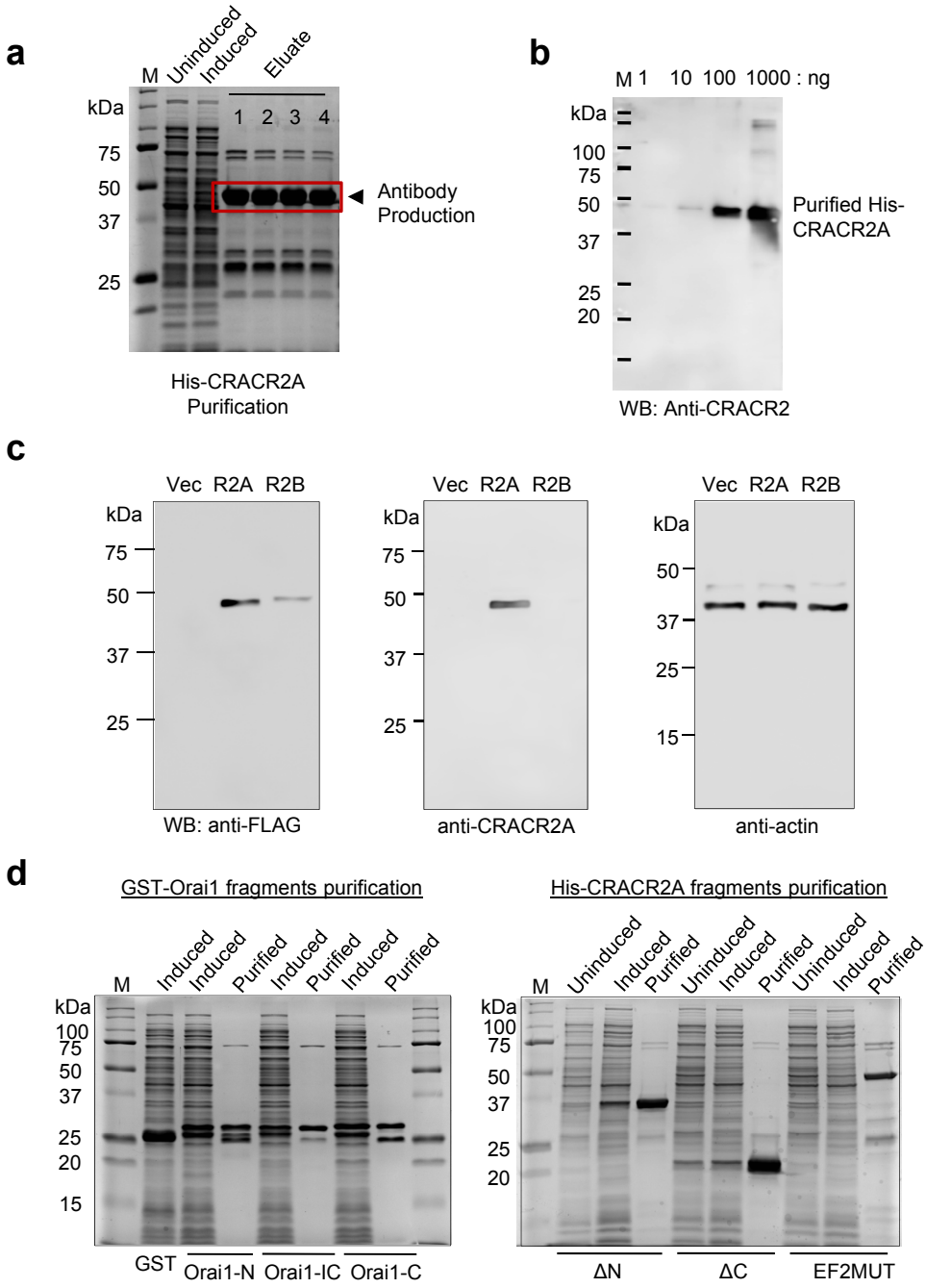

Figure S4 Purification of recombinant CRACR2A and Orai1 proteins and generation of anti-CRACR2A antibodies. (**a**) *E. coli* expressing 6X His-tagged CRACR2A proteins were either left uninduced or induced with 0.2 mM IPTG, and lysates were analyzed for CRACR2A expression. Eluates show purified CRACR2A protein (red box). The purified protein bands were excised to generate anti-CRACR2A antibody. Proteins were detected by coomassie blue staining. (**b**) Polyclonal antibody against CRACR2A generated in rabbits was examined for sensitivity to detect purified CRACR2A protein.(**c**) Examination of specificity of CRACR2A antibody. Lysates from HEK293 cells expressing either empty vector (Vec), CRACR2A, or CRACR2B were examined by immunoblotting with anti-FLAG antibody to detect both proteins (left), with CRACR2A antibody that detects only CRACR2A protein (middle panel), and with anti-actin antibody (right panel) as a loading control. (**d**) Lysates of *E.coli* expressing either GST or the N terminus (Orai1-N), the intracellular loop (Orai1-IC) or the C-terminus (Orai1-C) of Orai1 were separated by SDS-PAGE (labeled as induced) together with purified fragments (labeled as purified) and visualized by coomassie blue staining (left). Lysates of *E.coli* expressing 6X His-tagged truncation or point mutants of CRACR2A proteins were analyzed by SDS-PAGE and coomassie blue staining (right). Uninduced, induced cell lysates and proteins purified using Ni^{2+} resins were examined. M, molecular weight marker.

a

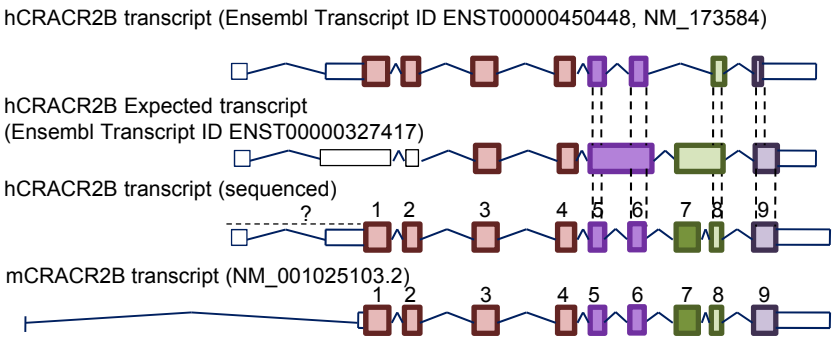

b

atggccagccctggaaagcctggggctgatgaggcccaggaggaggaggggaactcgaggggggctctgcagggccgcgggctgcaatactggagcaggctgaggagctgtttctgctgtgtgacaaggaggcta
agggcttcatcaccaagcacgacctgcagggtctccagagcgacctgcccctcacgccagagcagctggaggctgtgtttgaaagtctggaccgggctcacactggcttcctcaccgccagggagttctgcctgggcctgg
ggatgtttgtgggggtggcgtcagcccagggagcgaaccctgcaggactcccgaggagaccttgagtcgggcgggctcgacgtgcagggcacggcgggctctctggatgaggaggaggaagaggaggagcgattc
cacactgtgctggagcagctgggggtggccccggtcctgggcaagcagcgggctgtgaggacgctctgggccaggctgcagcgcgagcgccccgagctgctgggctctttcgaggatgttctgatacgcgcgtcggcctg
cctggaggaggcggcccgggagcgcgacggcctggagcaggcgctgcggaggcgcgagagcgagcacgagagggaggtgcgcgctctgtacgaggagacggagcagcttcgggagcagagccggcgcccgc
cgagtcagaacttcgcccgcggggagcggagaagccgtctggagctggagctgcagagccgcgagcaggacctggaacgcgcgggcctgcggcagcgggagttagagcagcagctgcacgcccaggctgcgga
gcacctggaggcacaggcccagaactcccagctgtggcgggcgcacgaggcgctgcgaacgcagctggaggggcgcaggagcagatccgcaggctggagagcgaagcacgaggccgccaggagcaaaccc
aacgagacgtggtcgccgtctccaggaacatgcagaaagagaaagtcagcctgctacggcaactggagctgctcagggagctgaatacacggctgcgggatgacagggacgcctgcgaggccaggcgggcgggca
gcagctgcaggaaggctctgacaacagcccgcctgcctgggcccacctgctgctgctgttgctgggctcggccccccagacgcggctctggccaccttcccagtgcccggtga

c

hCRACR2B	sequenced clone
mCRACR2B	NP_001020274

```
                                                    42 EF hand 1 53
hCRACR2B        MASPGKPGADEAQEEEGELEGGSAGPRAAILEQAEELFLLCDKEAKGFITKHDLQGLQSD 60
mCRACR2B        MASPGLPGSGEGQEGE-ETTGVSARHGVEVLQQAQELFLLCDKDAKGFITRQDLQGLQSD 59
                ***** **:.*.** * *  * **   . :*:**:********:*******::******** 

                                  76 EF hand 2 87
hCRACR2B        LPLTPEQLEAVFESLDRAHTGFLTAREFCLGLGMFVGVASAQGANPCRTPEETFESGGLD 120
mCRACR2B        LPLTPEQLEAVFESLDQAHTGFLTAREFCLGLGKFVGVESAPGGSPLRTSEETFESG--- 116
                ****************:**************** **** ** *..* **.******* 

hCRACR2B        VQGTAGSLDEEEEEEERFHTVLEQLGVAPVLGKQRAVRTLWARLQRERPELLGSFEDVLI 180
mCRACR2B        ---TGGSLEEEEEDVETFYTSLEKLGVARVLGEQWAVRTLWVGLQRERPELLGSLEEVLM 173
                   *.***:****: * *:* **:**** ***:* ******. ***********:*:**: 

                                  Coiled-coil
hCRACR2B        RASACLEEAARERDGLEQALRRRESEHEREVRALYEETEQ-LREQSRRPPSQNFARGERR 239
mCRACR2B        RASACLEAAAREREGLEQALRRRESEHEREVRGLYEELEQQLGEQRHRRQSQNLPREEQR 233
                ******* *****:******************.**** ** * ** :*  ***:.* *:* 

hCRACR2B        SRLELELQSREQDLERAGLRQRELEQQLHAQAAEHLEAQAQNSQLWRAHEALRTQLEGAQ 299
mCRACR2B        GHLELELQTREQELERAGLRQRELEQQLQARAAEQLEAQAQHIQLQRAYEAIRAQLDQAQ 293
                .:******:***:***************:*:***:******: ** **:**:*:**: ** 

hCRACR2B        EQIRRLESEARGRQEQTQRDVVAVSRNMQKEKVSLLRQLELLRELNTRLRDDRDACEARR 359
mCRACR2B        EQLSRLEGEAQGRQEQTQRDVVAVSRNMQKEKLSLLRQLELLRELNLRLRDERDACETKL 353
                **: ***.**:*********************:************* ****:*****:: 

hCRACR2B        AGSSCRKALTTARLPGPTCCCCCC-WARPPRRGSGHLPSAR 399
mCRACR2B        LGSSHRKALAIAHKPGPIYCCCCCGWARPPRRGSGHLPSAR 394
                 *** ****: *: ***  ***** ***************
```

Figure S5 Exon/intron architecture and cDNA sequence of human CRACR2B. (**a**) Top two schematics represent the exon/intron map of human CRACR2B transcripts. Bottom two schematics show the exon/intron map of the human CRACR2B mRNA cloned from Jurkat T cells in comparison with that of mouse CRACR2B (NM_001025103.2). The mRNA sequence of the cDNA we cloned is not identical to any predicted transcripts but showed high similarity with the sequence of mouse CRACR2B. The 5′ UTR sequence is not validated and is marked as a dotted line. (**b**) The nucleotide sequence of human CRACR2B cDNA cloned and sequenced from Jurkat T cells. The start and stop codons are indicated in red. (**c**) Amino acid sequence alignment of human CRACR2B (cloned from Jurkat T cells) and mouse homologue. Amino acid sequences were aligned using ClustalW2 (default options). The predicted Ca^{2+} binding EF-hands in the N terminus are colored in light blue. The residues in red indicate variable regions in the C terminus of CRACR2B that differ significantly with the amino acid sequences of CRACR2A. The predicted coiled-coil region using COILS is boxed in gray.

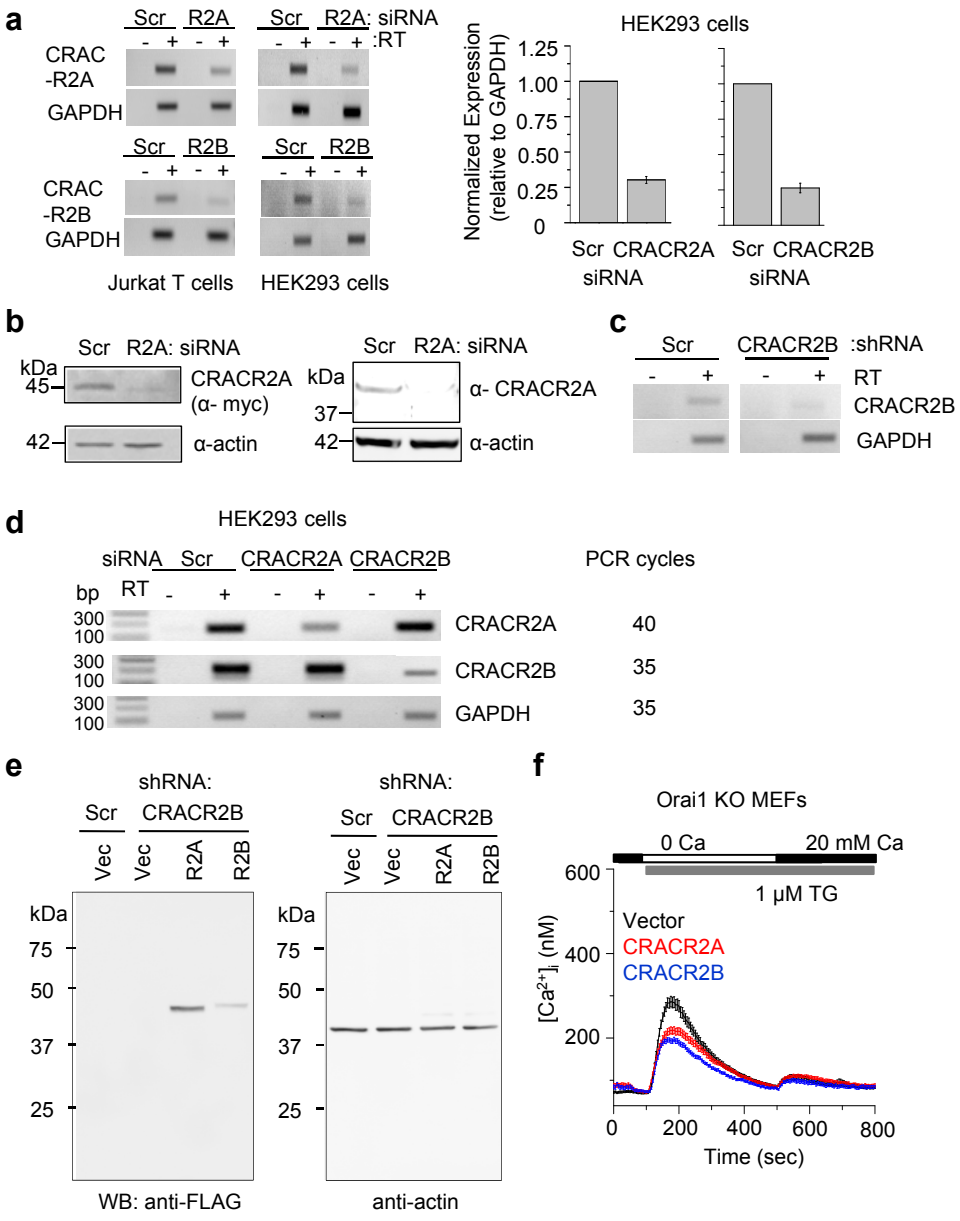

Figure S6 Knockdown efficiency of siRNAs and shRNAs targeting CRACR2A and CRACR2B in Jurkat T cells and HEK293 cells. (**a**) Jurkat T cells and HEK293 cells were transfected with siRNAs targeting CRACR2A or CRACR2B. The mRNA levels were visualized by agarose gel electrophoresis (left) and quantified (bar graph) using Multi-Gauge software (Fuji film). GAPDH-normalized mRNA levels are plotted relative to those in control cells. In HEK293 cells, CRACR2A transcripts were amplified using higher PCR cycles (40 as compared to 35 for all the other samples). RT stands for addition of reverse transcriptase during cDNA synthesis. (**b**) HEK293 cells stably expressing Myc-CRACR2A were transfected with scrambled siRNA (Scr) or siRNA targeting CRACR2A. Subsequent analysis of CRACR2A expression using immunoblot with anti-Myc antibody shows decreased CRACR2A expression in siRNA treated cells (left). Jurkat T cells transfected with control or CRACR2A-targeting siRNA were examined by immunoblotting using anti-CRACR2A antibody (right). Immunoblots with anti-actin antibody were used as a loading control. (**c**) HEK293 cells stably expressing control (Scr) or CRACR2B-targeting shRNA were examined for expression of CRACR2B transcripts. (**d**) Cross reactivity of siRNAs targeting transcripts of CRACR2A and CRACR2B were examined in HEK293 cells. (**e**) HEK293 cells stably expressing shRNA were transfected with plasmids encoding FLAG-tagged CRACR2A or CRACR2B cDNAs and immunoblotted using anti-FLAG antibody (left panel). Vec depicts lysates from cells transfected with empty vector. (**f**) Orai1-null MEFs were transduced with retroviruses encoding empty vector, CRACR2A, or CRACR2B cDNAs and SOCE was measured. Each trace is average ± s.e.m of 25-35 individual MEFs.

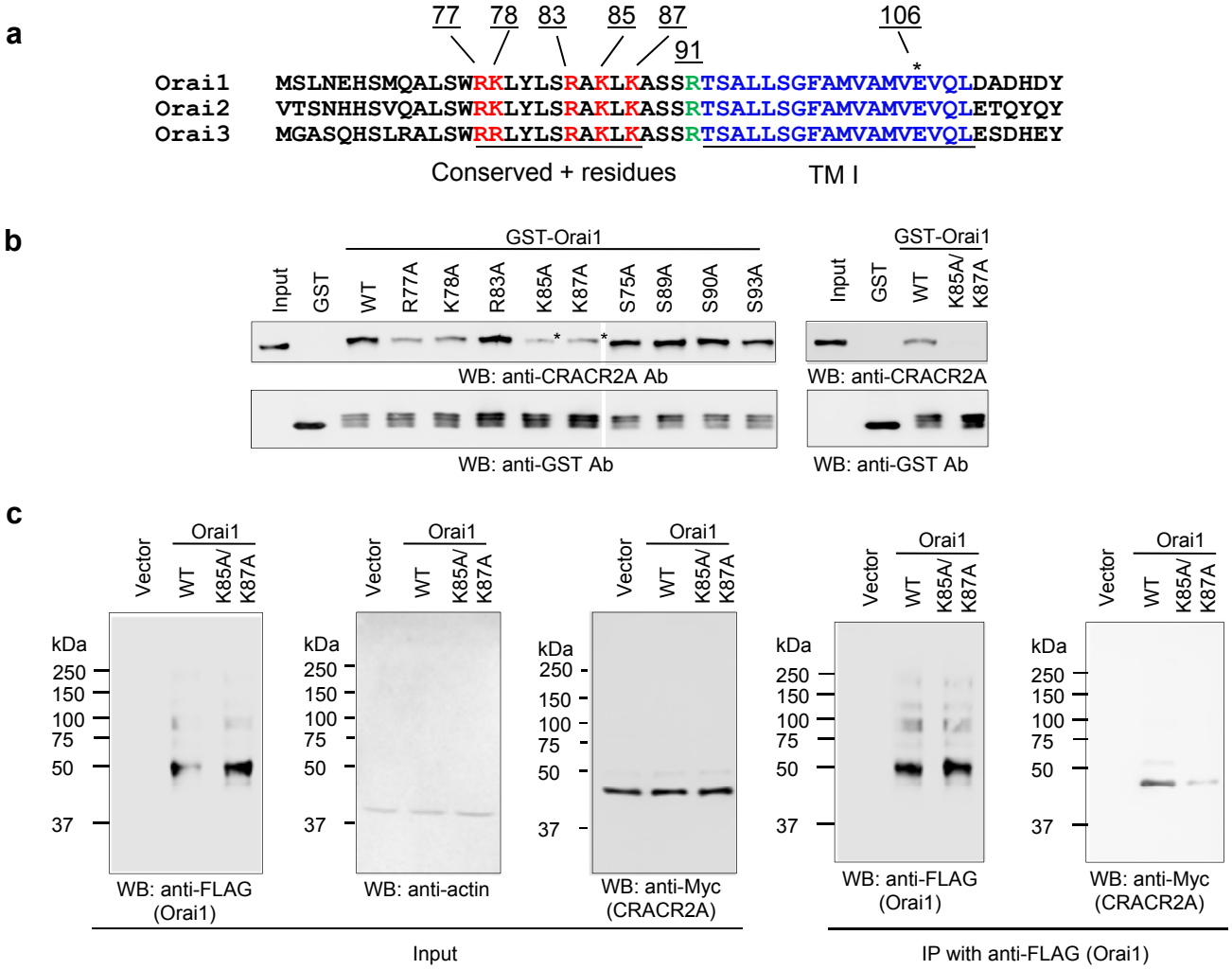

Figure S7 The positively charged residues K85 and K87 in the N terminus of Orai1 are important for interaction with CRACR2A. (**a**) Alignment of the N-terminal residues of human Orai proteins shows conservation of the positively charged lysine and arginine residues (labeled in Red). Arg91 (R91) is the residue mutated to Trp (R91W) in human SCID patients (green). The first transmembrane segment (TM I) and the pore residue, E106 are indicated in blue and asterisk (*), respectively. (**b**) GST pulldown assays with wild-type and mutant Orai1 N terminus fragments. In addition to the positively charged residues, the conserved serine residues were examined for their role in CRACR2A binding (left). Pulldown with the N terminus of Orai1$^{K85A/K87A}$ double mutant shows minimal binding to CRACR2A (right). Lower panels show the amount of GST fusion proteins using immunoblots. All the GST-fused WT, mutant Orai1 fragments, and full-length CRACR2A proteins were purified from *E. coli*. (**c**) HeLa cells stably expressing STIM1 were transfected with plasmids encoding Myc-CRACR2A together with either WT Orai1 or Orai1$^{K85/K87A}$ mutant. After 48 h, cells were treated with 1 μM thapsigargin, cross-linked with DSP and examined by immunoblotting for expression of WT Orai1, Orai1$^{K85/K87A}$ and CRACR2A (Input). Middle panel shows input levels using immunoblot with anti-actin antibody. After immunoprecipitation with anti-FLAG resin, precipitates were analyzed by immunoblotting with anti-FLAG and anti-Myc antibodies for detection of Orai1 and CRACR2A, respectively (IP).

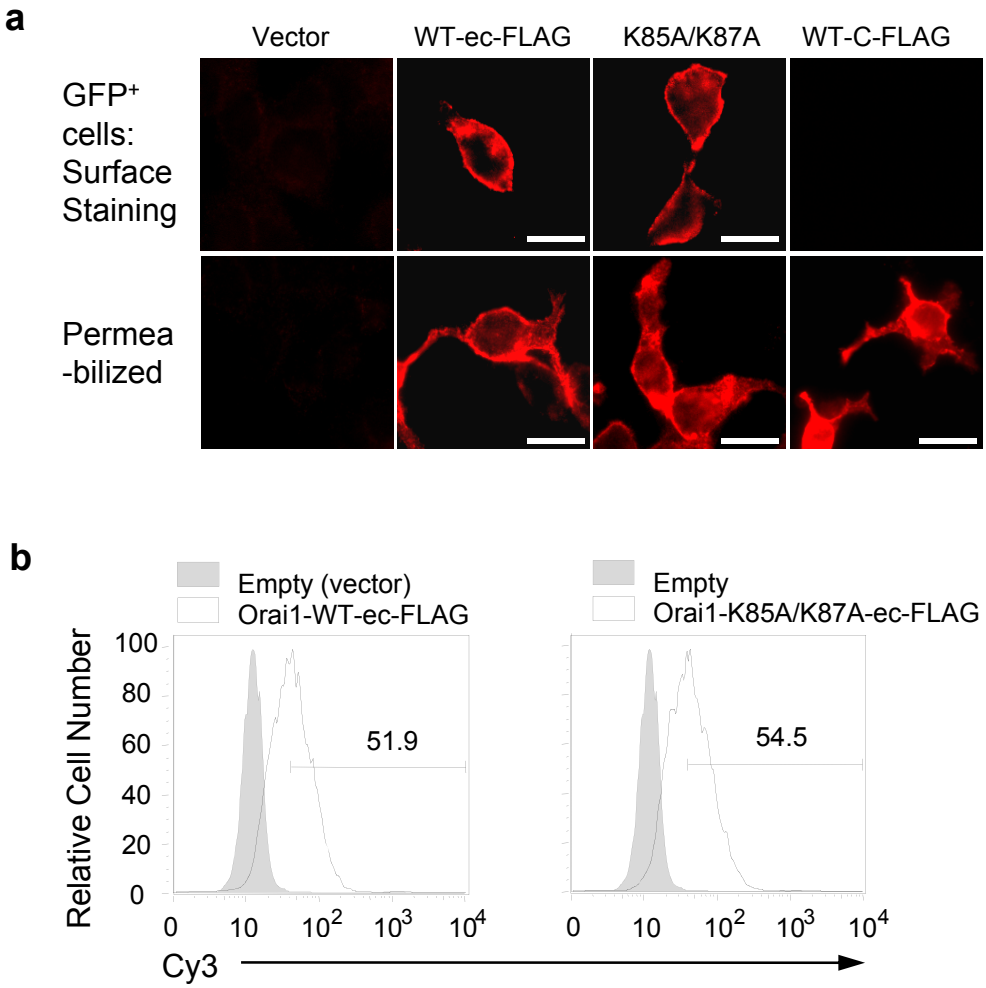

Figure S8 Examination of the expression levels of WT Orai1 and Orai1$^{K85A/K87A}$ proteins. (**a**) HEK293 cells expressing either wild-type (WT-ec-FLAG) or Orai1$^{K85A/K87A}$ mutant (K85A/K87A) with a FLAG epitope inserted between TM III and IV were left unpermeabilised (top panel) or permeabilised (bottom panel) and immunostained for detection of Orai1. As a control for surface staining, HEK293 cells were transfected with a plasmid encoding C-terminally FLAG-tagged Orai1 (WT-C-FLAG). Bar, 10 μm. (**b**) HEK293 cells expressing either WT or Orai1$^{K85A/87A}$ mutant were permeabilized, stained for Orai1, and examined using flow cytometry. Since this plasmid also expressed GFP from IRES site, only GFP^{+} population was gated for analysis. At least 30,000 events were collected for each sample.

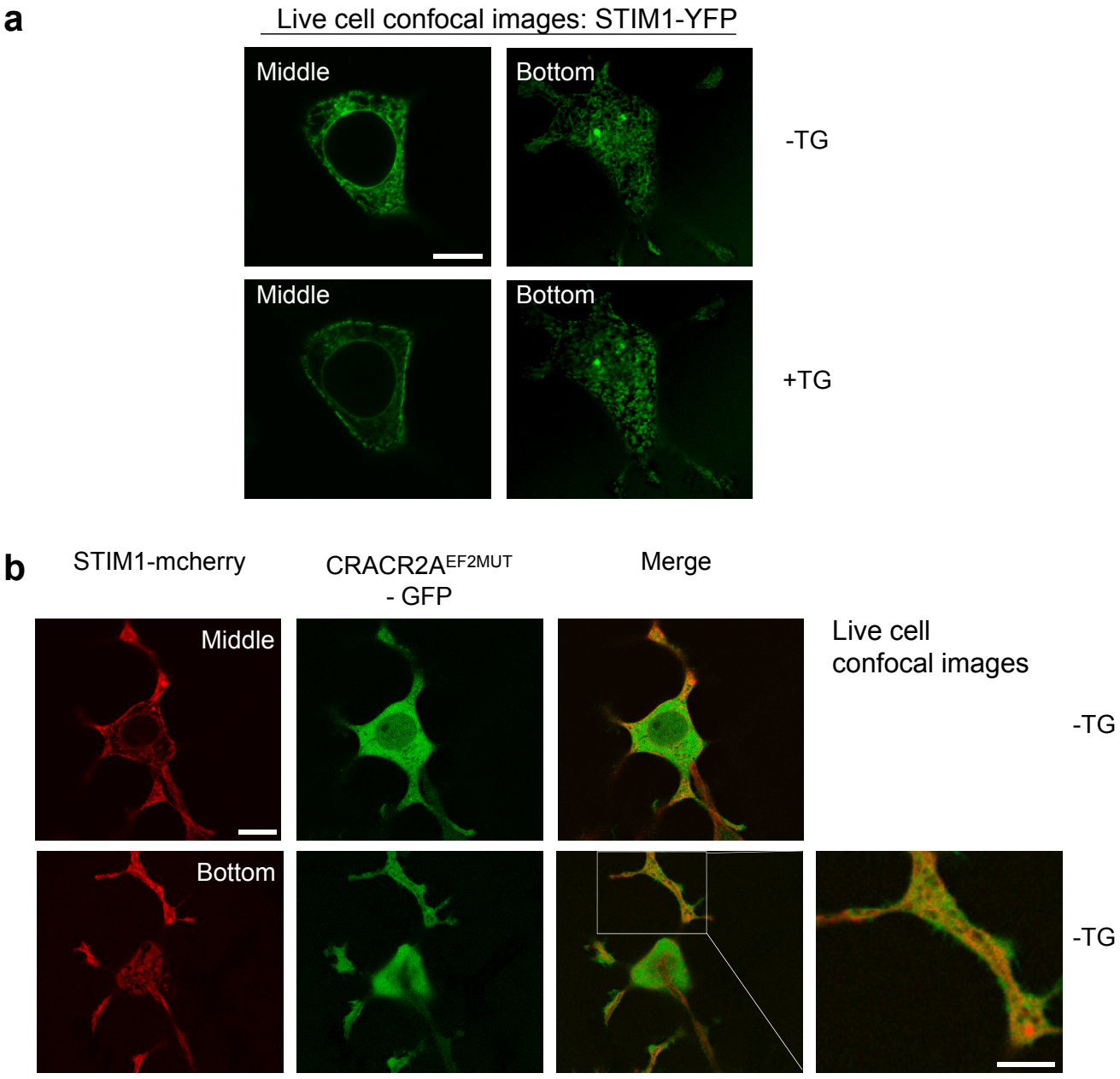

Figure S9 Co-expression of CRACR2A^{EF2MUT} enhances clustering of STIM1. (**a**) Live cell confocal microscopy of a HEK293 cell expressing STIM1-YFP shows localization of STIM1 before (-TG) and after store depletion (+TG) using 1 μM thapsigargin. Left panels show images of cell from the middle while right panels shows images from the footprint of the cell to visualize STIM1 clusters. Bar, 5μm. (**b**) Live cell confocal microscopy of a HEK293 cell expressing STIM1-mCherry with CRACR2A^{EF2MUT}-GFP shows partial co-localization of STIM1 and CRACR2A from the middle and bottom of the cell without store depletion. Bar, 5 μm. Scale bar in the magnified inset represents 2 μm.

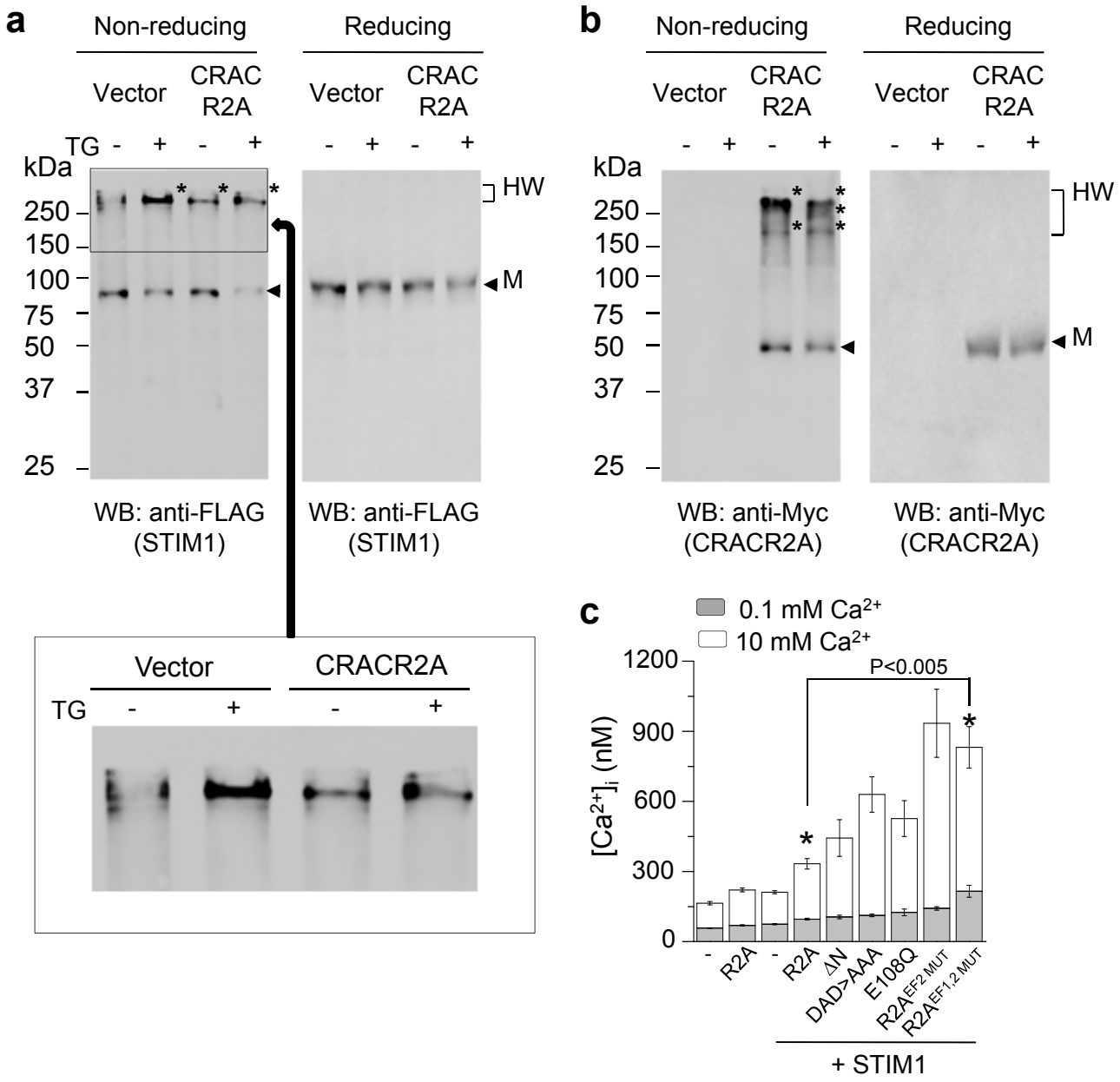

Figure S10 Co-expression of CRACR2A induces formation of high MW protein complex of STIM1. HEK293 cells expressing FLAG-STIM1 and Myc-CRACR2A were left untreated or treated with thapsigargin and cross-linked for 1 h using 0.1 mM DSP. After lysis, cellular extracts were cleared by ultracentrifugation, separated by SDS-PAGE under non-reducing or reducing conditions and immunoblotted using anti-FLAG (STIM1, **a**) or anti-Myc (CRACR2A, **b**) antibodies. Magnified inset shows distinct high MW protein bands (HW, indicated as *) of STIM1 after store depletion and presence of similar bands in the samples from cells overexpressing CRACR2A without store depletion. Immunoblots under reducing conditions serve as loading controls for STIM1 and CRACR2A. M indicates the monomeric form. (**c**) Measurement of cytoplasmic [Ca^{2+}] in the absence of ER Ca^{2+} depletion. HEK293 cells expressing STIM1 along with various CRACR2A mutants were examined for cytoplasmic Ca^{2+} in the presence of Ringer solution containing 0.1 or 10 mM $CaCl_2$ ions. * indicate samples with statistically significant differences in 0.1 and 10 mM Ca^{2+} containing solution ($P < 0.005$ by t-test). Data represent average ± s.e.m from three independent experiments.

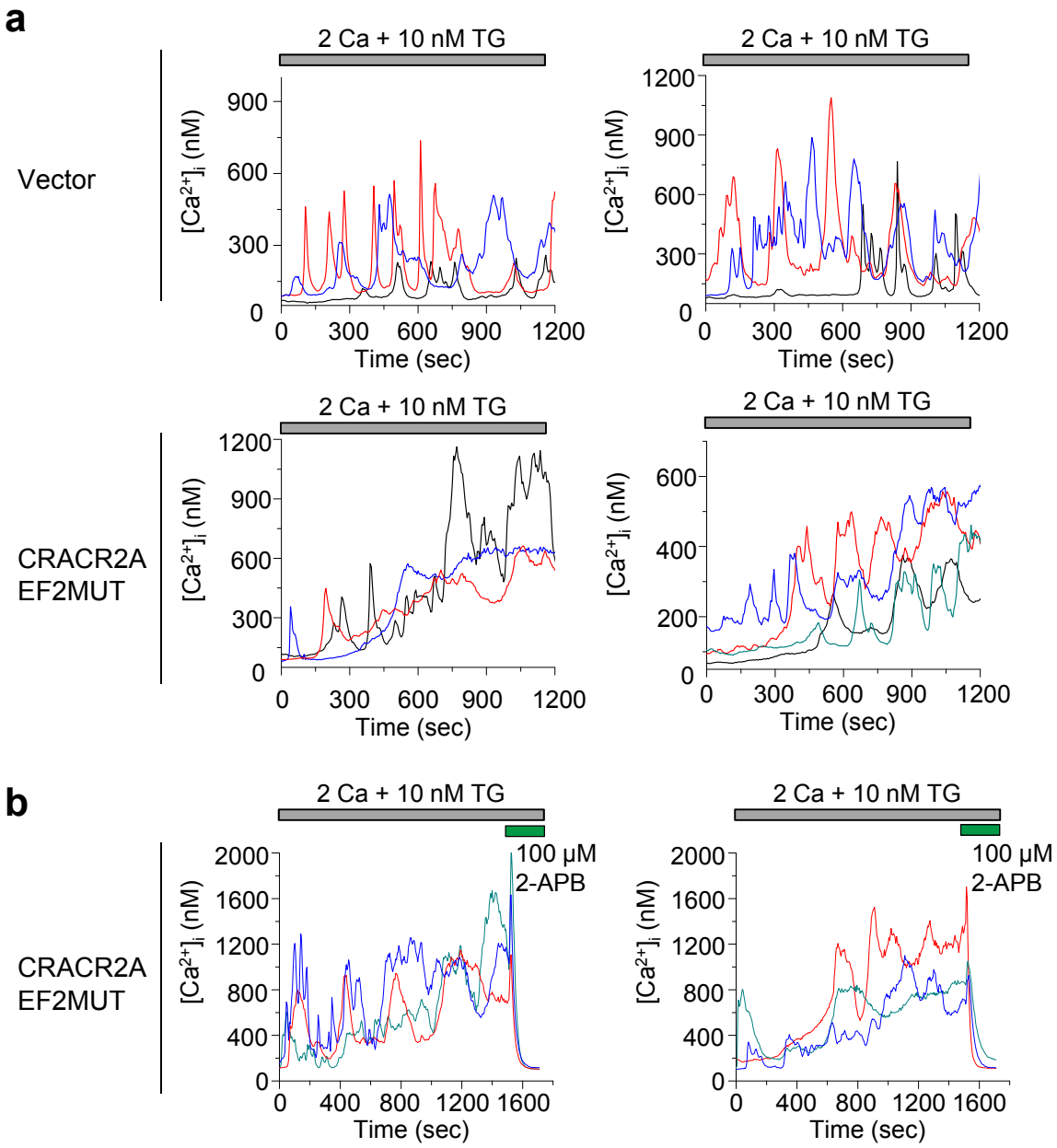

Figure S11 Expression of CRACR2A^{EF2MUT} in Jurkat T cells disrupts Ca^{2+} oscillations induced by CRAC channels. (**a**) Jurkat T cells expressing mCherry (Vector) or mCherry-fused CRACR2A^{EF2MUT} were treated with 10 nM thapsigargin in the presence of 2 mM external Ca^{2+} solution to induce asynchronous $[Ca^{2+}]_i$ oscillations. Graphs show raw traces of representative individual cells expressing either the empty vector (top, n = 6) or CRACR2A^{EF2MUT}-mCherry (bottom, n =7). (**b**) Addition of 100 μM 2-APB inhibits oscillations induced by 10 nM thapsigargin in Jurkat cells expressing CRACR2A^{EF2MUT}. Raw traces of 6 representative individual cells expressing CRACR2A^{EF2MUT} are shown.

Fig. 1b

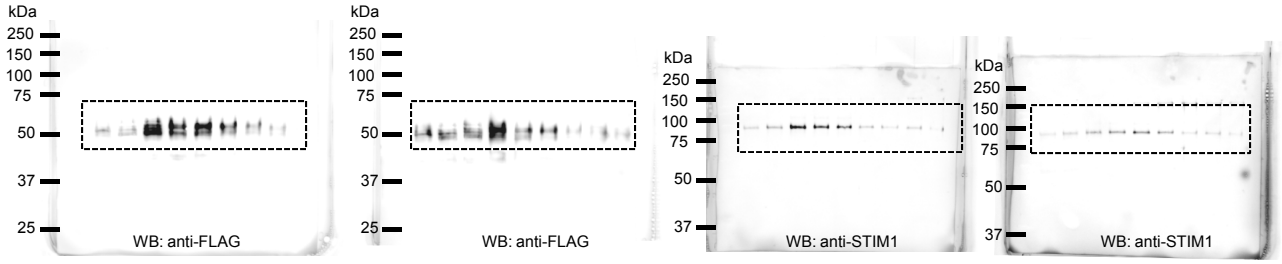

Fig. 2a, left

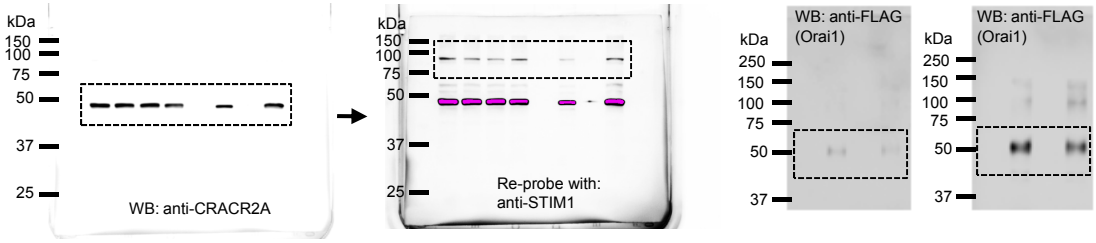

Fig. 2a, right

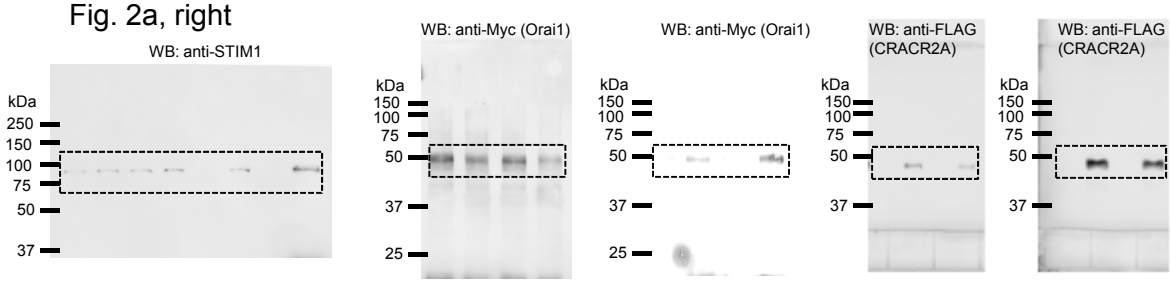

Fig. 2b, left

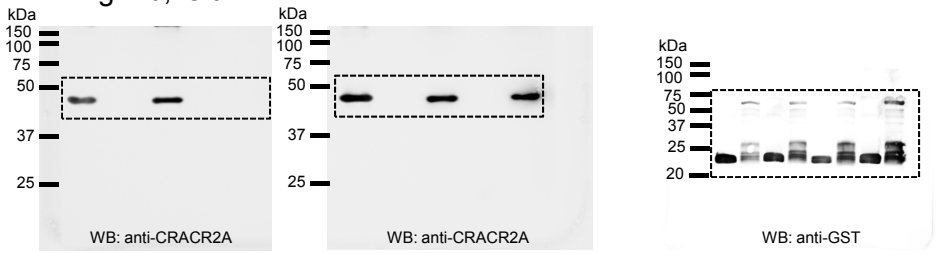

Fig. 2b, right

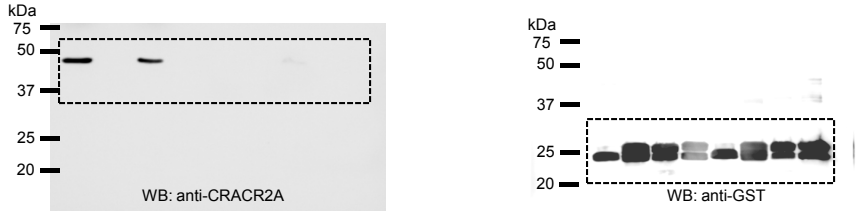

Figure S12 Full scans of key western blot data

Fig. 2c

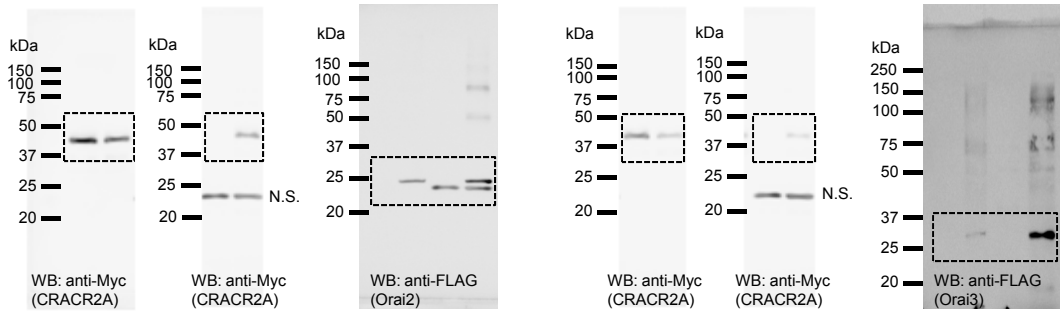

Fig. 2d

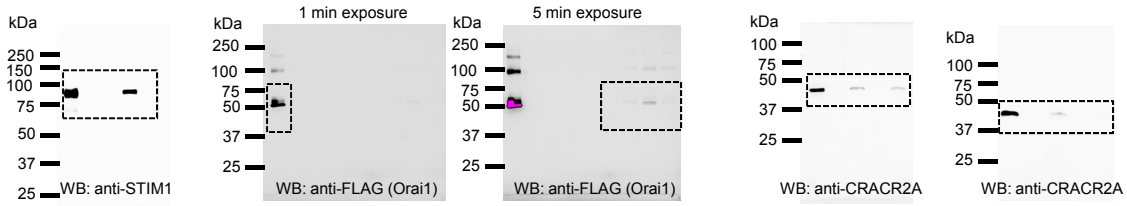

Suppl. Fig. 7b

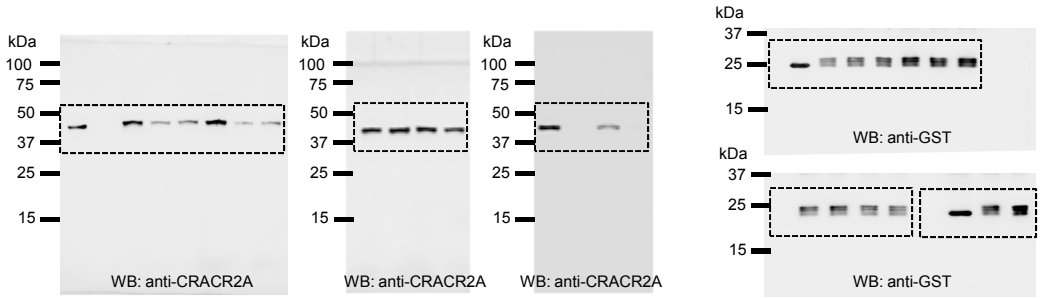

Figure S12 Continued

Supplemental Table 1.

Clone name	Forward Primer Sequence	Reverse Primer Sequence	PCR template
pEGFP-N1-CRACR2A	CGC CTC GAG ATG GCT GCC CCT GAC GGG AGG	CTG CAG AAT TCG GAC TGG TCC TTC CGA CCC CAG	CRACR2A in pCDNA3.1 myc his vector
pEGFP-C1-CRACR2A	AGA TCT CGA GCT ATG GCT GCC CCT GAC GGG AGG	GCA GAA TTC TCA GAC TGG TCC TTC CGA CCC	CRACR2A in pCDNA3.1 myc his vector
pmCherry-N1-CRACR2A			Cut the CRACR2A fragment from pEGFP-N1-CRACR2A and ligate to pmCherry-N1.
pEYFP-N1-STIM1	CGC CTC GAG ATG GAG GTA TGC GTC CGT CTT	CTG CAG AAT TCG CTT CTT AAG AGG CTT CTT AAA	STIM1 in pcDNA3.1 vector
pmCherry-N1-STIM1			Cut the STIM1 fragment from pEYFP-N1-STIM1 and ligate to pmCherry-N1.
CRACR2A ΔN (deletion of first 118 amino acids)	GCC CTC GAG ATG AGC CAG AAT AAC CCA AGT CAG	GTC AGC GGC CGC GAC TGG TCC TTC CGA CCC CAG	CRACR2A in pCDNA3.1 myc his vector
CRACR2A ΔC (deletion of last 128 amino acids)	CGC CTC GAG ATG GCT GCC CCT GAC GGG AGG	GTC AGC GGC CGC TTC GCC CAT GTC GCC CAG ATC	CRACR2A in pCDNA3.1 myc his vector
CRACR2A$^{63DAE>AAA}$ (CRACR2A^{EF1Mut})	TTC TTT CAG ACC TGT GCT GCT GCA GGC AAG GGC TTC ATC	GAT GAA GCC CTT GCC TGC AGC AGC ACA GGT CTG AAA GAA	CRACR2A in pCDNA3.1 myc his vector
CRACR2A$^{97DAD>AAA}$	GTG TTT GAT GCC CTG GCT GCT GCT GGC AAT GGC TAT CTG	CAG ATA GCC ATT GCC AGC AGC AGC CAG GGC ATC AAA CAC	Site directed mutagenesis (SDM) using WT CRACR2A cDNA as PCR template
CRACR2A^{E108Q}	TAT CTG ACC CCA CAG CAG TTC ACT ACTGGA TTT	AAA TCCAGT AGT GAA CTG CTG TGG GGT CAG ATA	SDM using WT CRACR2A cDNA as PCR template
CRACR2A$^{97DAD>AAA,E108Q}$ (CRACR2A^{EF2MUT})	TAT CTG ACC CCA CAG CAG TTC ACT ACTGGA TTT	AAA TCCAGT AGT GAA CTG CTG TGG GGT CAG ATA	SDM using CRACR2A$^{97DAD>AAA}$ cDNA as PCR template
pGEX 4T-1 CRACR2A	CGC GAA TTC ATG GCT GCC CCT GAC GGG AGG	GCG CTC GAG GAC TGG TCC TTC CGA CCC CAG	CRACR2A in pCDNA3.1 myc his vector
pGEX4T-1 WT Orai1 N-terminal fragment (amino acids 64-98)	CCG GAA TTC ATG AGC CTC AAC GAG CAC TCC	CCG CTC GAG GCC GGA GAG CAG AGC CGA GGT	pcDNA3.1 myc his-hOrai1
PCR of human CRACR2A	CTT CAG CCA GAA TAA CCC AAG TCA GG	TTT GGG CTC CAA GTC TGT CCA TCA	
PCR of human CRACR2B	CTG ATG AGG CCC AGG AGG AGG A	AGC CTC CTT GTC ACA CAG CAG AAA	
PCR of human GAPDH	ATC GTG GAA GGA CTC ATG ACC ACA	AGA GGC AGG GAT GAT GTT CTG GA	
PCR of mouse CRACR2A	AGA ACG AAC TGG AAT GTG CCC TCA	TCC TCT GCT TCT GAT TGA GTC GCT	
PCR of mouse CRACR2B	GCA GGA GCA AAC CCA AAG AGA TGT	AAT AGC TAG AGC CTT CCT GTG GCT	
PCR of mouse GAPDH	TGG AGA TTG TTG CCA TCA ACG ACC C	TAG ACT CCA CGA CAT ACT CAG CAC CG	